NeuroImage 170 (2018) 373–384

Contents lists available at ScienceDirect

NeuroImage

journal homepage: www.elsevier.com/locate/neuroimage

Defining the most probable location of the parahippocampal place area using cortex-based alignment and cross-validation

Kevin S. Weiner[a,*], Michael A. Barnett[a], Nathan Witthoft[a], Golijeh Golarai[a], Anthony Stigliani[a], Kendrick N. Kay[b], Jesse Gomez[c], Vaidehi S. Natu[a], Katrin Amunts[d,f,g], Karl Zilles[d,e,g], Kalanit Grill-Spector[a,h]

[a] Department of Psychology, Stanford University, Stanford, CA 94305, United States
[b] Department of Radiology, University of Minnesota, Minneapolis, MN 55455, United States
[c] Stanford Neurosciences Program, Stanford University School of Medicine, Stanford, CA 94305, United States
[d] Institute of Neurosciences and Medicine (INM-1), Research Centre Jülich, Jülich, Germany
[e] Dept. of Psychiatry, Psychotherapy and Psychosomatics, RWTH Aachen University, Aachen, Germany
[f] C. & O. Vogt Institute for Brain Research, Heinrich-Heine University Düsseldorf, Düsseldorf, Germany
[g] JARA-BRAIN, Jülich-Aachen Research Alliance, Jülich, Germany
[h] Stanford Neurosciences Institute, Stanford University, Stanford, CA 94305, United States

ARTICLE INFO

Keywords:
Parahippocampal place area
Scene perception
Collateral sulcus
Lingual sulcus
High-level visual cortex
Cortical folding

ABSTRACT

The parahippocampal place area (PPA) is a widely studied high-level visual region in the human brain involved in place and scene processing. The goal of the present study was to identify the most probable location of place-selective voxels in medial ventral temporal cortex. To achieve this goal, we first used cortex-based alignment (CBA) to create a probabilistic place-selective region of interest (ROI) from one group of 12 participants. We then tested how well this ROI could predict place selectivity in each hemisphere within a new group of 12 participants. Our results reveal that a probabilistic ROI (pROI) generated from one group of 12 participants accurately predicts the location and functional selectivity in individual brains from a new group of 12 participants, despite between subject variability in the exact location of place-selective voxels relative to the folding of parahippocampal cortex. Additionally, the prediction accuracy of our pROI is significantly higher than that achieved by volume-based Talairach alignment. Comparing the location of the pROI of the PPA relative to published data from over 500 participants, including data from the Human Connectome Project, shows a striking convergence of the predicted location of the PPA and the cortical location of voxels exhibiting the highest place selectivity across studies using various methods and stimuli. Specifically, the most predictive anatomical location of voxels exhibiting the highest place selectivity in medial ventral temporal cortex is the junction of the collateral and anterior lingual sulci. Methodologically, we make this pROI freely available (vpnl.stanford.edu/PlaceSelectivity), which provides a means to accurately identify a functional region from anatomical MRI data when fMRI data are not available (for example, in patient populations). Theoretically, we consider different anatomical and functional factors that may contribute to the consistent anatomical location of place selectivity relative to the folding of high-level visual cortex.

Introduction

The parahippocampal place area (PPA) is a functional region of the brain that responds more strongly to images of scenes and places compared to other classes of visual stimuli and is critical for scene and place recognition, as well as navigation (Aguirre et al., 1998; Epstein and Kanwisher, 1998; Epstein, 2008). Typically, the PPA is defined from functional magnetic resonance imaging (fMRI) experiments. The PPA is located within a gross anatomical territory that contains several macroanatomical structures including the collateral sulcus (CoS), the lingual sulcus, (LS), and the parahippocampal gyrus (PHG; Aguirre et al., 1998; Avidan et al., 2002; Epstein and Kanwisher, 1998; Epstein, 2008; Levy et al., 2004; Nasr et al., 2011; Weiner and Grill-Spector, 2010; Weiner et al., 2010). These macranatomical structures span several centimeters, making it hard to precisely predict the exact location of place selectivity from cortical folding patterns alone, which

* Correspondence to: Department of Psychology, Stanford University, Stanford, California 94305, United States.
E-mail address: kweiner@stanford.edu (K.S. Weiner).

http://dx.doi.org/10.1016/j.neuroimage.2017.04.040
Accepted 17 April 2017
Available online 18 April 2017

was nicely summarized in a recent review (Epstein, 2014).[1] A question remains whether it is possible to accurately identify the most probable location of these place-selective voxels without needing to acquire functional MRI data. Such a feat would be especially useful in patient populations and other participant groups in which it may be relatively easy to acquire anatomical data, but difficult to acquire functional data.

Of course, the identification of the PPA is complicated by (at least) four methodological considerations. First, the PPA definition may depend on the type of experiment, task, and stimuli used. Second, the boundaries of the PPA may depend on the statistical threshold used. Third, the spatial extent and localization of the PPA may vary if defined within the native brain space of an individual or based on a group analysis. Fourth, the size of the PPA may depend on data acquisition choices (e.g. large vs. small voxels) and data analysis choices (e.g. liberal smoothing vs. no spatial smoothing). The present study aims to identify and to predict the most probable location of place-selective voxels within medial VTC of an individual brain that is impervious to these methodological decisions.

To achieve this goal, the present study implemented a three-fold approach. First, we generated a probabilistic group ROI of place-selective voxels using cortex-based alignment (Fischl et al., 1999). Second, we quantified how well this probabilistic ROI predicts the location of the PPA, as well as place-selective fMRI responses, from an independent experiment and a separate set of participants. Third, we tested if this probabilistic ROI also captures the locus of highest place selectivity in (a) our data and (b) a separate set of data collected from over 500 participants by other researchers using different stimuli, tasks, and methods (shared from Nasr et al., 2014 and the Human Connectome Project, Barch et al., 2013).

The results from these analyses demonstrate that (a) the anatomical location of place-selective voxels relative to cortical folding is consistent across participants, (b) the probabilistic ROI identifies the location of the PPA in individual brains from multiple independent datasets, and (c) the probabilistic ROI encapsulates voxels in medial VTC exhibiting the highest place selectivity in our data as well as shared data from other labs. Our probabilistic ROI of place selectivity is freely available with this study aligned to the FreeSurfer average cortical surface (vpnl.stanford.edu/PlaceSelectivity).

Materials and methods

Participants

To identify place-selective voxels, 12 adults (5 females) participated in fMRI Study 1 and 12 independent adults (8 females) participated in fMRI Study 2. Procedures were approved by the Stanford Internal Review Board on human participants research.

Study 1

Functional localizer

12 adults participated in 4 runs of an fMRI functional localizer experiment (6 min/run; from Stigliani et al., 2015; http://vpnl.stanford.edu/fLoc/). Each run consisted of 16 s blocks, which contained different images from the same category presented at a rate of 1 Hz. Images within each block were from one of 5 different categories: faces (adult and child faces), places (corridors and houses), bodies (limbs and headless bodies), characters (numbers and pseudowords), and objects (cars and guitars). The view, size, and retinal position of the images varied. Each item was overlaid on a 10.5° phase-scrambled background generated from a randomly selected image from the entire set to minimize low-level differences across categories. We controlled for low-level differences such as contrast, luminance, similarity to other stimuli of the same category, and spatial frequency (for further details, please see: http://vpnl.stanford.edu/fLoc/). Participants performed an oddball task during which they were instructed to fixate on a central dot and detect an oddball phase scrambled image that occurred randomly within the blocks. The incidence of the oddball image was 0, 1, or 2 times per block.

Data acquisition

Participants were scanned at the Center for Neurobiological Imaging (CNI) at Stanford University using a 3 T GE scanner equipped with a custom-built phase-array, 32-channel head coil. We acquired 34 slices covering occipitotemporal cortex (resolution: 2.4×2.4×2.4 mm; one-shot T2*-sensitive gradient echo acquisition sequence: FOV=192 mm, TE=30 ms, TR=2000 ms, and flip angle=77°).

Study 2

Functional localizer

12 adults (8 females) participated in two runs during which they viewed gray-scale natural images of faces (children and adult faces), objects (abstrack objects and cars), places (indoor scenes and outdoor scenes), and scrambled images (created by randomly scrambling pictures into 225, 8×8 pixel squares as in Golarai et al., 2010b and Golarai et al., 2015). Indoor scenes of buildings were mostly of empty rooms and corridors, devoid of furniture. Outdoor scenes were of natural settings that were (with a few exceptions) devoid of buildings. All scenes were devoid of people, animals, or salient objects. Stimuli were presented at a rate of 1 Hz in 12 s blocks followed by 12 s of a blank screen with a central red fixation dot. As described previously (Golarai et al., 2015), low-level differences among images were assessed using pixel-wise similarity. Participants performed a 1-back task during which they were instructed to fixate on the central red dot and to press a button whenever they detected identical images appearing successively, which occurred on ~17% of the images per block.

Data acquisition

Participants were scanned at the Lucas Imaging Center at Stanford University in a 3 T GE scanner equipped with an 8-channel surface coil. We acquired 32 slices at a resolution of 3.125×3.125×3 mm using a two-shot T2*-sensitive spiral (Glover, 1999) acquisition sequence (FOV=200 mm, TR=2 s, TE=30 ms, and flip angle=76°).

Neuroanatomical data for Studies 1and 2

Data acquisition

A standard high-resolution anatomical volume of the whole brain was acquired using either a T1-weighted SPGR pulse sequence (TR=1000 ms, flip angle=45°, 2 NEX, FOV=200 mm, resolution: 0.78×0.78×1.2 mm) or a T1-weighted BRAVO pulse sequence (TR=450 ms, flip angle=12°, 1 NEX, FOV=240 mm, resolution: 1.0mm isotropic). For consistency, the former data were resampled to 1.0 mm isotropic.

Cortical surface reconstruction

All anatomical volumes were aligned to the AC-PC plane. Using automated (FreeSurfer: http://surfer.nmr.mgh.harvard.edu) and manual segmentation tools (ITK-SNAP: http://www.itksnap.org/pmwiki/pmwiki.php), each anatomical volume was segmented to separate gray from white matter, and the resulting boundary was used to reconstruct the cortical surface for each subject (Wandell et al., 2000).

[1] Specifically, Epstein eloquently and accurately defines these issues: "The PPA is a functionally defined, rather than an anatomically defined region. This can lead to some confusion, as there is a tendency to conflate the PPA with parahippocampal cortex (PHC), its anatomical namesake. Although they are partially overlapping, these two regions are not the same. The PPA includes the posterior end of the PHC but extends beyond it posteriorly into the lingual gyrus and laterally across the collateral sulcus into the fusiform gyrus." (Epstein, 2014, pp.107)

Data analyses

Data from Study 1 and Study 2 were analyzed with MATLAB using the mrVista toolbox (http://github.com/vistalab) as in our prior publications (Weiner and Grill-Spector, 2010, 2011; Golarai et al., 2010a, 2010b; Stigliani et al., 2015). AS and KW analyzed the data and defined functional regions of interest (ROIs) in Study 1. GG and NW analyzed the data and defined functional ROIs in Study 2.

Time series processing

For Study 1 and Study 2, functional data from each session were motion corrected using an affine transformation (Nestares and Heeger, 2000). Time series data were processed with a temporal high-pass filter (1/20 Hz cutoff) and then converted to percentage signal change by dividing the time series of each voxel by its mean intensity. We estimated the blood oxygen level dependent (BOLD) response amplitudes for each condition using a general linear model (GLM) applied to the time series of each voxel using as predictors the experimental conditions convolved with the hemodynamic impulse response function used in SPM. Data were not spatially smoothed.

Functional region of interest (fROIs)

Place-selective voxels were defined within each subject's native brain anatomy using a common threshold ($t > 3$, voxel-level) for both Studies 1 and 2. Study 1 compared BOLD responses to images of places (corridors and houses) relative to images of faces (adult and child faces), bodies (limbs and headless bodies), characters (numbers and pseudowords), and objects (cars and guitars). Study 2 compared BOLD responses to images of places (indoor scenes and outdoor scenes) relative to images of faces (children and adult faces) and objects (abstract objects and cars). Though there are some overlapping categories between Studies 1 and 2, the exemplars representing each category were different between studies. There was no difference in the surface area of these regions across experiments (a 2-way ANOVA with hemisphere and experiment as factors yielded no effect of hemisphere ($F(1,44)=2.8$, $p=0.1$), no effect of method ($F(1,44)=1.22$, $p=0.3$), and no interaction ($F(1,44)=0.2$, $p=0.7$). The average surface area (± SEM) across experiments was 599 ± 39 mm^2 and 518 ± 83 mm^2 in the right and left hemisphere, respectively. Prior studies have identified a gradient of place selectivity in parahippocampal cortex in which more anterior voxels illustrate higher place selectivity compared to more posterior voxels (Baldassano et al., 2013; Grill-Spector et al., 2000; Grill-Spector, 2003; Grill-Spector and Malach, 2004; Silson et al., 2016). The present study focuses on the more anterior cluster because (1) it can be anatomically and functionally differentiated from the more posterior cluster (Grill-Spector et al., 2000; Grill-Spector, 2003; Grill-Spector and Malach, 2004) and (2) the two clusters may artificially appear contiguous in some participants due to large draining veins (Vu and Gallant, 2015).

Sulcal definitions in medial VTC

To best understand the location of place selectivity relative to cortical folding, an accurate identification of sulci in medial VTC is imperative. Contrary to historical (Huschke, 1854; Retzius, 1896) and modern definitions of a single lingual sulcus (LS), Mangin and colleagues (Mangin et al., 2015) recently identified an anterior intralingual sulcus (S. Li. Ant.) and a posterior intralingual sulcus (S. Li. Post.). We used 84 brains (73 living and 11 postmortem, none of which were used for our functional analyses) to examine the morphology of the LS. We used postmortem brains in addition to those from living individuals as the classic examinations were from postmortem brains. Cortical surfaces were generated for each postmortem brain using methods that are detailed in prior publications (see Lorenz et al., 2017; Caspers et al., 2013; Weiner et al., 2014, 2017 for details). We

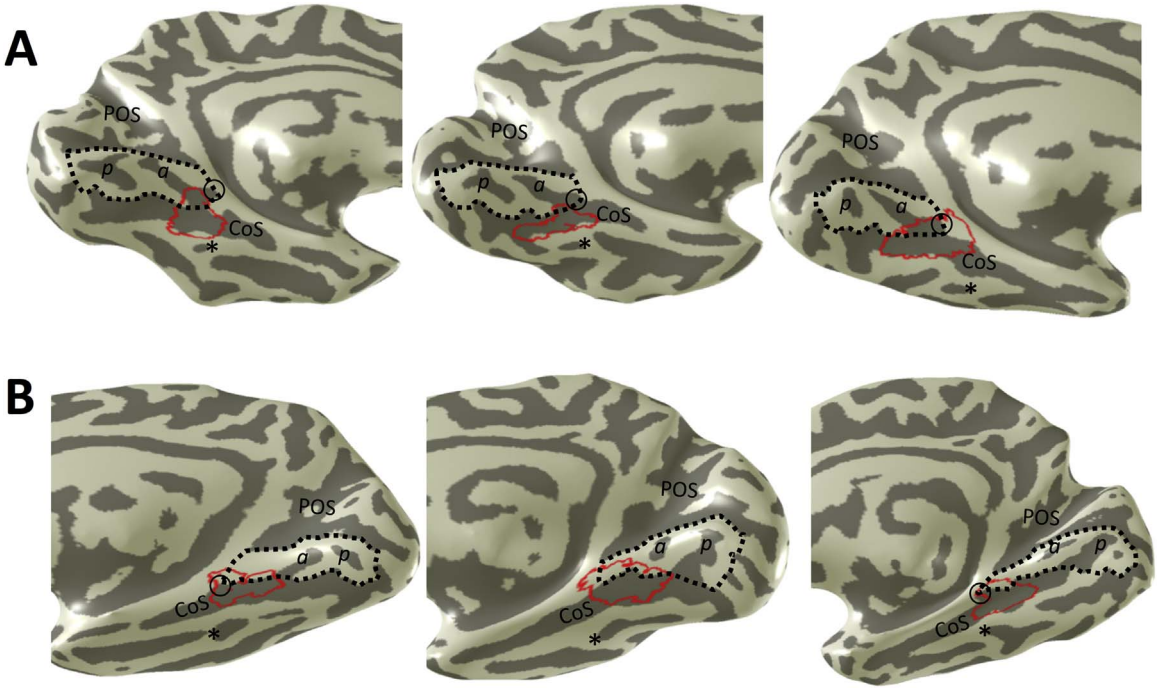

Fig. 1. The location of place-selective voxels relative to the folding of medial ventral temporal cortex in individual subjects. Cortical surface reconstructions zoomed on medial ventral temporal cortex in left (A, top) and right (B, bottom) hemispheres. Place-selective voxels (bounded by the red contour) are consistently located within the banks of the collateral sulcus (CoS). There is variability as to how much place-selective voxels extend into the lingual (dotted black line; LG) and parahippocampal gyri (PHG). The CoS-ph (circle) is a small branch, or ramus, of the CoS dividing the LG from the PHG (Ono et al., 1990). It is more easily identifiable on the pial surface and is not always identifiable on inflated cortical surfaces (for example, only in 5 of out of the 6 depicted hemispheres). *a:* anterior lingual sulcus (ALS). *p*: posterior lingual sulcus (PLS). POS: parietal occipital sulcus. *Asterisk:* anterior tip of the mid-fusiform sulcus.

replicated the identification of two lingual sulci in 86.7% (146/168) of hemispheres independent of whether or not the brain was from a living or postmortem individual (Figs. 1 and 2). The anterior (ALS) and posterior (PLS) lingual sulci separate the LG into anterior, mid, and posterior components. Interestingly, the ALS intersects with the occipital branch of the CoS (CoS-o; Petrides, 2012) in almost twice as many cases in the left (67.9%) compared to the right (36.9%) hemisphere. This hemispheric difference is also evident in the FreeSurfer (FS) template, which is an average of 39 different adult brains (Fig. 2). What we refer to as the ALS has also been referred to as the Sulcus paracollateralis (Smith, 1907), the subcalcarine fissure (Wilder, 1901), the intralingual ramus of the CoS (Ono et al., 1990), and the medial CoS-o (Huntgeburth and Petrides, 2012; Petrides, 2012). We agree with Mangin and colleagues to define this sulcus as the anterior lingual sulcus rather than a medial branch or ramus of the CoS because it is located within the LG.

Generating a group probabilistic region of interest (pROI) of place selectivity

We generated separate probabilistic ROIs from the 12 participants in Study 1 and the 12 participants in Study 2. These probabilistic ROIs were generated using cortex-based alignment (CBA) tools in FreeSurfer (Fischl et al., 1999; http://surfer.nmr.mgh.harvard.edu/). Briefly, the cortical surface of each of our 12 participants was aligned to the FreeSurfer average surface (from 39 healthy adults not used in our study) using a high-dimensional nonlinear registration algorithm. Using this alignment, we transformed functional ROIs (fROIs) from each subject to the FreeSurfer (FS) average brain. Probabilistic maps (Fig. 2) were then generated by summing the 12 fROIs at each point along the cortical surface of the FS average brain and dividing by the number of participants. Each vertex within the map reflects the proportion of participants exhibiting place selectivity at that location on the cortical surface. Probabilistic ROIs were generated in three ways: (1) unthresholded, (2) thresholded by 33% overlapping participants, or (3) thresholded by 66% overlapping participants. We used these three different thresholds to test if and how different threshold values influence the predictability of place selectivity in a new group of participants. Based on related work (Weiner et al., 2017), a threshold of 0.33 is sufficient for predicting functional ROIs in VTC. The pROI from Study 1 was previously published (Weiner et al., 2017).

Assessing the correspondence between the probabilistic ROI and individually-defined ROIs in independent participants

Using data from Study 1, we generated three probabilistic ROIs as described above. Using data from Study 2, we used CBA to align each subject's cortical surface to the FS average brain and then used the same transformation to project fROIs from each individual subject to the FS average brain. Because these individual fROIs were in the same common space as the probabilistic ROI from Study 1, we could compare their spatial locations on the cortical surface.

We calculated the Dice coefficient to determine how well our probabilistic ROIs from Study 1 predicted each individually-defined ROI from Study 2 on the FS average brain. The Dice coefficient is calculated with the following formula:

$$Dice\ Coefficient = \frac{2|P \cap A|}{|P| + |A|},$$

where P is the surface area of the probabilistic ROI and A is the surface area of the actual ROI in an individual subject. We repeated this calculation for the probabilistic ROI generated from Study 2 and the individual subject fROIs from Study 1 (Fig. 2C). We repeated this calculation an additional time with an exhaustive leave-one-out cross validation procedure using data from all 24 participants and then compared our calculations to results using Talairach alignment (Fig. 2D; see *Comparing our predictions using CBA to volume-based, Talairach alignment*).

Perfect alignment between the probabilistic prediction and the actual ROI in individual subjects would result in a Dice coefficient of 1 and complete misclassification would result in a Dice coefficient of 0. We calculated a ceiling (the empirically best dice coefficient given the noise in the data) performance as the Dice coefficient between the probabilistic ROI in Study 1 and each individual subject from Study 1 that contributed to generating the probabilistic ROI from the same experiment. We repeated this estimate of the ceiling performance for Study 2 as well. The ceiling performance plotted in Fig. 2 (horizontal gray bar) is the average of the two estimates.

We tested if there were differences in the predictability of fROIs across studies using a 2-way ANOVA with study and hemisphere as factors. There was no effect of study ($F(1,44)=0.3$, $p=0.68$), no effect of hemisphere ($F(1,44)=1.43$, $p=0.24$), and no interaction ($F(1,44)=1.43$, $p=0.61$). Thus, results in Fig. 2 are the average across the two different approaches (e.g. predicting individual ROIs in Study 2 from a probabilistic ROI from Study 1 and vice versa).

Comparing our predictions using CBA to volume-based, Talairach alignment

A common procedure in the field is to align functional data to an anatomical template in stereotaxic coordinate space such as Talairach space (Talairach and Tournoux, 1988). Prior work shows that functional regions in high-level visual cortex are better aligned to one another after CBA compared to stereotaxic alignment (Frost and Goebel, 2012). Thus, we repeated our leave-one-out cross-validation procedure across all 24 participants with an affine volume-based registration to the Talairach brain and compared this performance to the same procedure implemented with CBA in FreeSurfer (Fig. 2D).

Testing the functional profile of probabilistic predictions

In addition to examining the ability of the probabilistic ROI to spatially predict the actual ROI in individual subjects, we also examined if the voxels in this probabilistic ROI displayed significantly higher BOLD responses to places compared to other stimuli. To do so, we used CBA to project the probabilistic ROI generated from Study 1 on the FS average brain to the native brain space of each subject from Study 2. We then extracted response amplitudes from this ROI to each of the stimuli shown in Study 2 in each individual subject and tested whether this ROI exhibited stronger responses to places compared to other stimuli (Fig. 3).

Examining the topological relationship between the probabilistic ROI and peak place selectivity in medial VTC in over 500 participants

In addition to identifying the most probable location of place-selective voxels in medial VTC, we also tested whether or not our pROI captured voxels that exhibit the highest (sometimes referred to as 'peak') place selectivity in medial VTC in new participants. Here, we define 'peak' as those voxels with the highest selectivity as indicated by the t-statistic. To address this question, we examined if the probabilistic pROI contains (a) peak place-selective voxels within medial VTC in individual participants from our data (24 participants, Fig. 4), (b) the group average peak selectivity across 24 participants from our data (Figs. 4 and 5), (c) the cortical location of peak place selectivity from 247 participants from the Human Connectome Project (HCP) 500 Participants Release (Barch et al., 2013; Fig. 5), (d) the cortical location of peak place selectivity from a separate set of 247 participants from the HCP 500 Participants Release (Barch et al., 2013; Fig. 5), and (e) the cortical location of peak place selectivity from a separate set of 26 participants from a recent study by Nasr and colleagues (Nasr et al., 2014, Fig. 5). The data in Fig. 5c–e were preprocessed and analyzed with different methods than those implemented

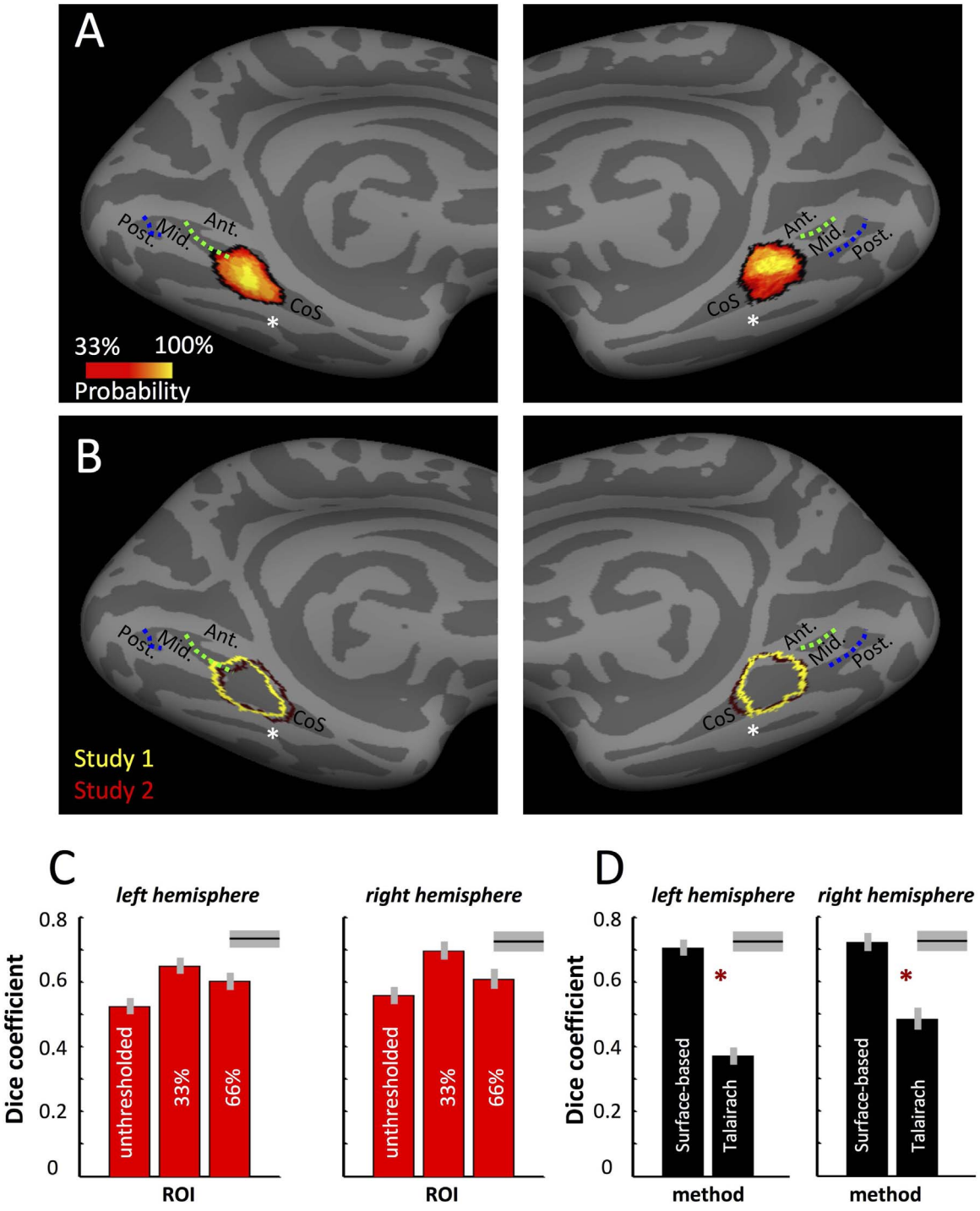

Fig. 2. Accurate predictions of place-selective voxels in medial VTC from probabilistic ROIs. (A) Probabilistic maps of place-selective voxels from 12 participants in Study 1. Maps of the right and left hemisphere on the FreeSurfer (FS) template reflect those voxels shared by at least four subjects. (B) Outline of the probabilistic ROIs (pROIs) from (A) in yellow relative to pROIs from Study 2 (maroon) from 12 new participants. *Blue:* posterior lingual sulcus; *Green:* anterior lingual sulcus; *Asterisk:* anterior tip of the mid-fusiform sulcus. (C) The correspondence between predicted and actual ROIs in individual subjects as assessed by the Dice coefficient for unthresholded, 33% thresholded, and 66% thresholded pROIs in the right and left hemispheres. The best possible fit in our data determined by ceiling performance is indicated by the horizontal gray bar in the top right. (D) A leave-one-out-cross-validation procedure in all 24 subjects across Studies 1 and 2 (at 33% threshold) compared the performance of cortex-based and volume-based alignment techniques (e.g. Talairach) to predict place-selective voxels in a left out participant. Cortex-based alignment out-performed volume-based Talairach alignment by nearly a factor of two in the right hemisphere (1.85 ± .26) and more than a factor of two in the left hemisphere (2.23 ± .24). * all ps < 10^{-6} Ant.: Anterior; Mid.: Middle; Post.: Posterior.

in Studies 1 and 2: the HCP data were analyzed by author KNK (see section *Analysis of place selectivity from the HCP 500 dataset*), while the data from Nasr and colleagues were shared as an overlay file in FreeSurfer representing a random effects analysis comparing static images of scenes to static images of objects in 26 participants (see Nasr et al., 2014 for details). Thus, this approach allows us to examine the topological relationship between our pROI and clusters of peak place selectivity from over 500 additional individuals.

It should be noted that there is a fundamental difference between the probability map of place-selective ROIs (Fig. 2) and the selectivity maps (Figs. 4 and 5). In particular, the map of pROIs across subjects is generated after assigning either a 1 (if the ROI is present) or a 0 (if the ROI is not present) at vertices of the FS average surface. On the contrary, the latter selectivity map reflects a continuous metric in which a vertex is assigned a selectivity value (for the present study, a t-statistic) first for each subject and then averaged across subjects. Thus, for the latter case, there is no threshold and the group map directly indicates selectivity (each vertex reflects the average t-value across subjects), while for the former case, there is a threshold and the group map does not reflect selectivity and instead represents the percentage of overlap across subjects at each vertex.

Analysis of place selectivity from the HCP 500 dataset

To identify the cortical locus of peak place selectivity from the HCP dataset, minimally pre-processed data of the HCP 500 Participants Release (Barch et al., 2013) were used to identify place-selective regions. Data from 494 participants were included in the download and analyzed using GLMdenoise (http://kendrickkay.net/GLMdenoise/; Kay et al., 2013). The GLM included four regressors to model experimental effects: one regressor for each combination of stimulus category (bodies, faces, places, tools) during the 0-back task. Beta weights were converted to units of percent signal change by dividing by the mean intensity at each gray coordinate. Participants were randomly split into two groups (N=247 in each group) in order to assess reliability of the effects. In each subject, we computed a contrast between the beta weight for places against the mean of the beta weights for bodies, faces, and tools. The resulting contrast map of each subject was aligned to the FS average cortical surface. We then averaged these contrast maps across participants on the FS average cortical surface, separately for each of the two groups of 247 participants. Clusters reflecting peak selectivity across subjects were generated using a threshold of $t > 2.5$, vertex level.

Results

Place-selective voxels in medial VTC are located in the banks of the CoS with inter-subject variability

Our data illustrate that macroanatomical features create a reliable set of landmarks that confine place selectivity in medial ventral temporal cortex (VTC), which replicates and extends previous findings (Aguirre et al., 1998; Epstein and Kanwisher, 1998; Nasr et al., 2011, 2014; Weiner et al., 2010; Weiner and Grill-Spector, 2010). For example, our data show that place-selective voxels are consistently located within the banks of the collateral sulcus (CoS) in individual participants (Fig. 1). Posteriorly, place-selective voxels seldom extend past the posterior tip of the anterior lingual sulcus (ALS; Materials and Methods for a description of the ALS and posterior (PLS) lingual sulcus). Anteriorly, place-selective voxels often macroanatomically align with the anterior tip of the mid-fusiform sulcus (MFS; asterisk in Fig. 1). Of course, this structural-functional coupling is not always perfect and there is inter-subject variability as to how much the place-selective voxels extend within the PHG, as well as the LG and medial aspects of the fusiform (FG) gyrus (Fig. 1; see also Supplemental Figs. 1–4 and Fig. 4). Nonetheless, despite this inter-subject variability, place-selective voxels are always located within the CoS across participants. The consistency between the identification of place-selective voxels and cortical folding suggests that it may be possible to use cortex-based alignment to generate a group probabilistic ROI that would predict the most probable location of place selectivity within VTC in independent participants.

Cortex-based alignment generates a group-based probabilistic ROI that maintains the structural-functional relationship between place selectivity and cortical folding

Using cortex-based alignment (CBA) tools in FreeSurfer (FS; Materials and Methods), we generated a probabilistic ROI (pROI) of place selectivity separately for each study. To determine the utility of this pROI: (1) we examined if the group pROI maintains the structural-functional coupling observed in individual participants, (2) we tested if the group pROI is stable across studies that used different methods, and (3) we used a cross-validation approach to quantify how well the pROI predicts the location of the actual ROI in a new group of participants.

Examining the location of the pROI generated from Study 1 on the FS average brain reveals that the macroanatomical location of the pROI (Fig. 2A) falls within the same series of anatomical landmarks we identified in individual participants. Furthermore, projecting the pROI from Study 2 on the FS average brain revealed a close correspondence between the pROIs across the two studies (Fig. 2B). To quantify how well pROIs predict functionally-defined ROIs in an independent group of participants, we used the Dice coefficient metric to calculate the amount of spatial correspondence between the two regions in individual brains (Materials and Methods). We did this analysis using group pROIs from Study 1 and individual ROIs from Study 2 and vice versa, measuring cross-validation performance at three threshold levels (no threshold, 33%, and 66%). The ceiling Dice coefficient in our data is 0.73 ± 0.03 in the left hemisphere and 0.72 ± 0.03 in the right hemisphere (as opposed to 1, which is the mathematically largest Dice coefficient; Materials and Methods).

The results of this cross-validation analysis reveal that our pROI predicts individual ROIs with high accuracy across hemispheres. At a threshold of 33%, the Dice coefficient is 0.70 ± 0.03 in the right hemisphere and 0.65 ± 0.03 in the left. The predictability of the pROI approached, but was significantly lower than, the ceiling performance in both hemispheres (all $ts > 3.3$, all $ps < 0.003$). Repeating these quantifications with both a more lenient pROI (an unthresholded ROI) as well as a more stringent ROI (a thresholded ROI at 66%) also revealed Dice coefficients larger than 0.5, with numerical values varying with threshold (Fig. 2C). The unthresholded ROI had the lowest predictability (right: 0.56 ± 0.03; left: 0.52 ± 0.03) and the 66% thresholded ROI had an intermediate predictability (right: 0.61 ± 0.03; left: 0.60 ± 0.03) - all of which were significantly lower than the ceiling performance (all $ts > 4.5$, all $ps < 10^{-4}$).

We also performed an exhaustive leave-one out cross validation (LOOCV) procedure using data from all 24 participants across both studies. That is, in each iteration, the pROI was first generated from 23 participants and then tested how well it predicted the left out, 24th participant. Since the 33% thresholded pROI performed the best in the prior analyses, we used this threshold for the present (and subsequent) analyses. Results again revealed high predictability (mean Dice coefficients in the right (0.72 ± 0.03) and left (0.70 ± 0.03) hemispheres), which was not different than the ceiling performance (all $ts < .7$, all $ps > .5$; Fig. 2D). Thus, cross-validated performance from 23 participants is not significantly different than the ceiling performance, which provides statistical evidence supporting that the structural-functional predictability from our participants likely reflects a predictability that is reflective of the general population (see Fig. 5). Together, these analyses reveal that the group pROI maintains the structural-functional coupling observed in individual participants and it is possible to predict the location of place-selective voxels in medial VTC from cortical folding alone.

Cortex-based alignment out-performs volume-based alignment by nearly a factor of two

Our previous work quantifying the relationship between cortical folding and face-selective regions showed that surface-based predictions out-performed predictions based on stereotaxic coordinates (Weiner et al., 2014). Nevertheless, predicting the location of place selectivity from stereotaxic coordinates may not be as impeded as face-selective regions due to the relatively medial location of place-selective voxels in the brain. To test this hypothesis, we repeated the exhaustive LOOCV procedure across 24 participants using Talairach-based alignment. We then compared the Dice coefficients between this approach and those resulting from CBA (using the pROI with the 33% threshold; see previous section). The mean Dice coefficients for the Talairach–based approach were 0.48 ± 0.04 and 0.37 ± 0.03 in the right and left hemispheres, respectively (Fig. 2D). These Dice coefficients were lower than CBA, as CBA out-performed Talairach alignment by nearly a factor of two in the right hemisphere (1.85 ± 0.26) and by a factor of more than two in the left hemisphere (2.23 ± 0.24). A 2-way ANOVA with factors of method and hemisphere yielded a main effect of method ($F(1,92)=98.6$, $p < 10^{-6}$), a main effect of hemisphere $F(1,92)=5.0$, $p < 0.03$), and no interaction ($F(1,92)=2.8$, $p=0.1$). Thus, the implementation of CBA significantly improved the alignment and predictability of place selectivity within medial VTC across participants compared to Talairach alignment.

Probabilistic ROI identifies voxels exhibiting highest BOLD responses to places in individual participants

To further test the effectiveness of our predictions, we extracted the response amplitudes from the pROI. To do so, we used CBA to project the pROI from Study 1 to each individual brain of the participants in Study 2. We then extracted the response amplitudes from the pROI in each individual subject. We used the 33% thresholded pROI, which produced the highest Dice coefficient in the previous analyses. As illustrated in Fig. 3, the predicted ROI exhibited significantly higher mean response amplitudes to indoor and outdoor scenes compared to cars, abstract objects, child faces, adult faces, and textures. Thus, as one would hope, the predicted place-selective ROI exhibits the expected higher response to places than other stimuli. A 2-way ANOVA with factors of hemisphere (right/left) and category (indoor place, outdoor place, car, abstract object, adult face, child face, texture) revealed a main effect of category ($F(6,154)=20.4$, $p < 10^{-6}$), no effect of hemisphere ($F(1,154)=2.8$, $p=0.1$), and no interaction ($F(6,154)=0.14$, $p=0.99$). Together, our probabilistic predictions identify voxels in medial VTC that illustrate higher response amplitudes for places than other stimulus categories (at least those tested in the present experiment).

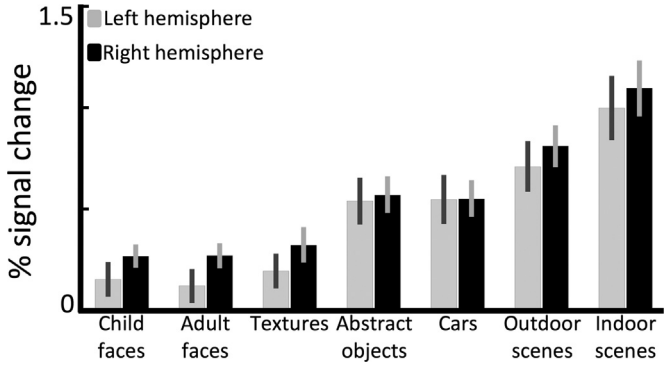

Fig. 3. Voxels predicted to be place-selective by Study 1 exhibit highest fMRI responses to images of scenes in Study 2. Mean fMRI responses (N=12) as a function of category are shown for Study 2. Predicted voxels exhibited higher fMRI responses to images of indoor and outdoor scenes compared to images from a variety of other categories. *Errorbars:* SEM.

Probabilistic ROI identifies the location of 'peak' place selectivity in over 500 participants

In addition to identifying the most probable location of place-selective voxels in medial VTC, which was the primary goal of the present study, a related experimental question is whether this pROI captures the 'peak' voxels exhibiting the highest place selectivity in medial VTC. To address this question, we first generated a group map of place selectivity across our 24 participants to visualize the locus of peak place selectivity across subjects and experiments used to generate the pROI. Here, we used CBA to generate an average map of selectivity in which vertices are assigned continuous values of place selectivity rather than a binary distinction as in the probability maps from the prior analyses. We then visualized the group place selectivity map relative to the group pROI from all 24 participants.

Fig. 4 shows an unthresholded group map of place selectivity (calculated from data across 24 participants from Studies 1 and 2) on the FS average brain relative to the outline of our pROI. Consistent with prior research (Baldassano et al., 2013; Epstein, 2008; Nasr et al., 2011; Silson et al., 2016) the group map illustrates place selectivity within the CoS, LG, PHG, the parietal occipital sulcus (POS), and retrosplenial cortex (RSC). Weakly (i.e. with t-values greater than 0 and less than 2) place-selective voxels do extend into the medial fusiform gyrus and more posteriorly along the CoS. Nonetheless, there is a consistent "hotspot," or locus, of peak place selectivity. Specifically, the locus of peak place selectivity is observed near the medial lip of the CoS in the right hemisphere and close to the center of our pROI near the fundus of the CoS in the left hemisphere (Fig. 4A). It is important to emphasize that the locus of peak place selectivity is within the group pROI (Fig. 4A-black contour).

Examining the location of our pROI relative to the peak cluster of place selectivity in individual participants shows that there are individual differences in the location of voxels with highest place selectivity (Fig. 4B-C). That is, voxels with the highest place selectivity are not always located within the same exact location in the pROI for each participant and small clusters of high place selectivity can also extend outside of the pROI. Nevertheless, despite these individual differences, all participants have voxels with the highest place selectivity within the pROI (Fig. 4B–C).

Crucially, our pROI not only identifies voxels exhibiting the highest selectivity in our own data, but also identifies voxels exhibiting the highest place selectivity in independent datasets from over 500 participants. These comparisons reveal two main results. First, the location of peak place selectivity occurs within the CoS in two separate splits (each consisting of data from 247 participants) from the HCP 500 subject release (Barch et al., 2013), as well as data from 26 participants from Nasr and colleagues (Nasr et al., 2014; Fig. 5). Second, even though there is variability in the exact location of peak selectivity across datasets, the locus of peak place selectivity across these experiments differing in stimuli, tasks, methods, and participants is located within our pROI. Altogether, our data and analyses suggest that our pROI of place selectivity is a robust predictor of the location of high place selectivity within medial VTC and these predictions are generalizable across data collected with different scanners, participants, images used for localization, data acquisition, and analysis methods.

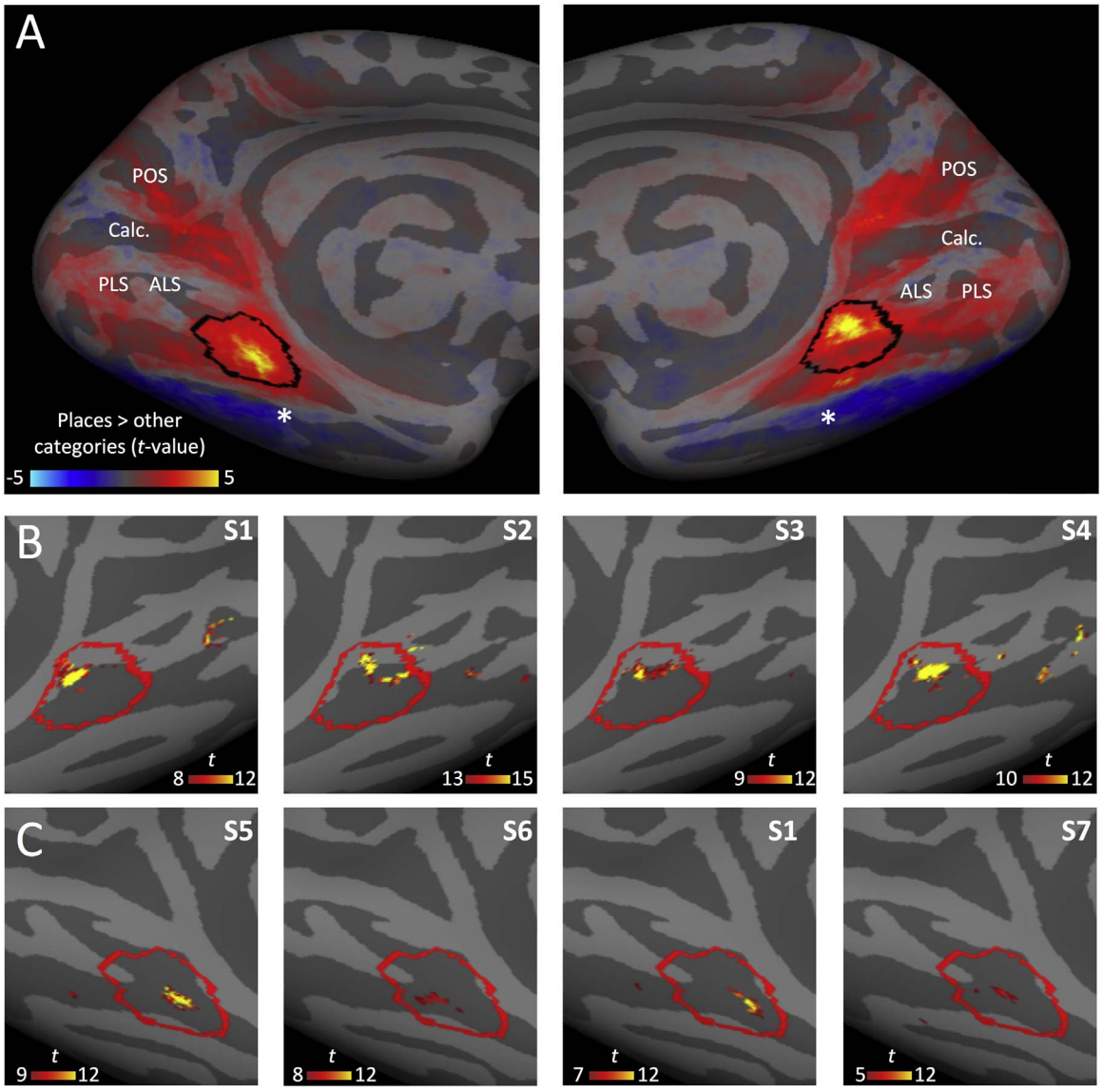

Fig. 4. Comparing the locus of peak place-selectivity relative to the probabilistic ROI (pROI). (A) An unthresholded map illustrating place-selectivity (places > other categories) averaged across all 24 subjects from Studies 1 and 2 on the FreeSurfer average cortical surface. Black outline illustrates the pROI across these 24 subjects defined with a 33% threshold. The most selective voxels are located within this pROI. *Left:* Left hemisphere. *Right:* Right hemisphere. *Asterisk:* anterior tip of the mid-fusiform sulcus. *ALS:* anterior lingual sulcus. *Calc:* calcarine sulcus. *PLS:* posterior lingual sulcus. *POS:* parietal occipital sulcus. **(B–C)** A thresholded map showing voxels exhibiting peak place selectivity in four example individual subjects. The colorbar indicates the thresholded value (left most number) to identify the peak in each subject. There is individual variability in the magnitude of peak selectivity, the exact location of peak selectivity, as well as additional small clusters located outside of our pROI. **(B)** Right hemisphere. **(C)** Left hemisphere.

Discussion

In this study, we examined the relationship between cortical folding patterns and the most probable location of place selectivity in medial ventral temporal cortex (VTC). Our results show that cortical folding patterns and probabilistic predictions reliably identify place-selective voxels in medial VTC across individuals and experiments. Below, we discuss these findings in the context of (1) predicting functional regions from cortical folding across the visual hierarchy and (2) anatomical/functional mechanisms that may contribute to this predictable relationship between cortical folding and place selectivity in medial VTC.

Predicting functional regions from cortical folding across the visual hierarchy

Our findings contribute to a growing body of work supporting a tight relationship between cortical folding and functional regions across the visual hierarchy. For example, V1 is reliably located within the calcarine sulcus (Henschen, 1893; Inouye, 1909). Additionally, intermediate visual areas are also located in consistent locations relative to cortical folding: V3A abuts and extends into the transverse occipital sulcus (Nasr et al., 2011; Tootell et al., 1997), the anterior boundary of human V4 is located within the posterior transverse collateral sulcus (Witthoft et al., 2014), and hMT+ is found at the intersection of the lateral occipital sulcus and the ascending branch of the posterior inferotemporal sulcus (Dumoulin et al., 2000). Likewise, several high-level category-selective regions have also been reported to be reliably located relative to cortical folding patterns. The fusiform face area is composed of at least two distinct regions (mFus-faces and pFus-faces), which are well predicted by the mid-fusiform sulcus (Weiner et al., 2014, 2017; Weiner and Grill-Spector, 2010, 2011, 2012, 2013; Weiner and Zilles, 2016; Grill-Spector and Weiner, 2014) and are also cytoarchitectonically dissociable (Weiner et al., 2017). The fusiform body area/OTS-limbs (Weiner and Grill-Spector, 2010, 2013)

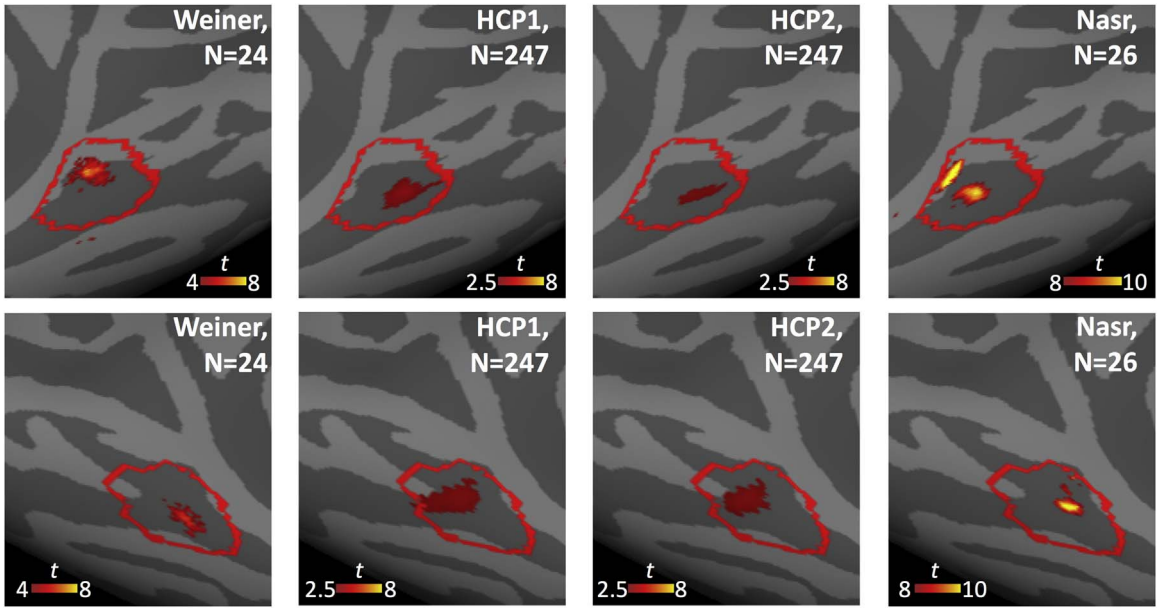

Fig. 5. The relationship between our probabilistic ROI (pROI) and the locus of place selectivity in over 500 participants. All panels show the FreeSurfer cortical surface zoomed in on ventral temporal cortex. *Red outline:* Contour of the pROI of place selectivity from 24 subjects in the present study. *Heat map:* thresholded place-selectivity map in a group of subjects from (left to right): (1) the present 24 subjects, (2) 247 subjects from one half of the Human Connectome Project 500 subject release, (3) 247 subjects from the other half of the Human Connectome Project subject release, and (4) 26 subjects from Nasr et al., 2014. Each map is stringently thresholded to isolate the cortical location of the most selective voxels in each independent group of participants. Note that the threshold and limits of the color bar are different for each group due to the differences in methods implemented across studies to localize functional selectivity. Despite these differences, the cortical location of voxels exhibiting peak place selectivity is within the pROI of the present study. *Top:* Right hemisphere; *Bottom:* Left hemisphere.

and the visual word form area are reliably found in the occipitotemporal sulcus (Ben-Shachar et al., 2007; Glezer and Riesenhuber, 2013; Stigliani et al., 2015; Wandell et al., 2012; Yeatman et al., 2013). Finally, the extrastriate body area is composed of at least three anatomically distinct regions that are localized to the lateral occipital sulcus (LOS-limbs), inferotemporal gyrus (ITG-limbs), and middle temporal gyrus (MTG-limbs; Weiner and Grill-Spector, 2011, 2013).

We extend these findings to now include a precise set of anatomical landmarks identifying place-selective voxels within medial VTC. Prior studies have reported place selectivity within the CoS (Epstein and Kanwisher, 1998; Levy et al., 2001; Levy et al., 2004; Nasr et al., 2011; Weiner and Grill-Spector, 2010; Weiner et al., 2010). Nevertheless, the CoS is very long – extending nearly across the entire length of the ventral portions of the occipital and temporal lobes. Our current findings provide a series of anatomical landmarks that constrain the location of place-selective voxels to a specific location along the CoS. In particular, the CoS/ALS junction is most predictive of place selectivity as illustrated by the convergence of place selectivity across studies in this location (Fig. 5). The tight coupling between cortical folding and place selectivity identified in the present study suggests that our pROI, which we share with the field, can predict place selectivity in the human brain with high likelihood using cortex-based alignment methods. This finding is consistent with other recent studies that showed that CBA improves the registration of functional data across participants (Benson et al., 2012, 2014; Frost and Goebel, 2012). Importantly, the use of our pROI does not necessitate the acquisition of functional MRI data, which we discuss further in the next section.

The utility of our probabilistic ROI (pROI) for localizing place-selective voxels when fMRI data are or are not available

We make our pROI freely available on the FreeSurfer (FS) average surface (vpnl.stanford.edu/PlaceSelectivity). This pROI can be used to localize place-selective voxels when fMRI data are not available. We have cross-validated our pROI across participants and studies including the identification of peak place selectivity in the CoS from data representing over 500 participants (Barch et al., 2013; Nasr et al., 2014). These data were collected with different voxel resolutions, stimuli, tasks, scanners, and analysis methods. Thus, our probabilistic ROI is generalizable across many different methodological decisions spanning experimental design, as well as fMRI data acquisition and analyses. However, this pROI is not perfect. We underscore that additional analysis decisions such as the statistical threshold used, the precise contrast, or the amount of spatial smoothing influence the spatial extent of the ROI on the cortical surface. As such, our pROI may not always identify the exact boundaries of the "PPA," but it will always identify the most probable location of voxels with the highest place selectivity within medial VTC. It should be noted that the cortical location of these voxels is consistent with recent definitions of the "anterior parahippocampal place area" (Baldassano et al., 2013; Silson et al., 2016) and CoS-places (Weiner et al., 2010; Stigliani et al., 2015). Additionally, as a recent study (Vu and Gallant, 2015) shows that the identification of place-selective voxels within medial VTC is affected by draining veins more so than other high-level regions in VTC such as face-selective regions, the use of our pROI to guide the localization of place-selective voxels in future studies may help to reduce variability induced by artifacts produced by large draining veins. We also emphasize that our pROI complements prior methods aimed to identify place-selective regions in VTC. For example, a prior approach (Julian et al., 2012) first anatomically identifies a large cortical expanse in parahippocampal cortex, then restricts this expanse to a smaller cortical extent that is place-selective when fMRI data are available. These approaches complement one another and achieve different research intentions: the approach by Julian and colleagues attempts to automate the identification of the PPA from fMRI data, while the present approach aims to identify the most probable location of place-selective voxels in VTC based on anatomical data even when fMRI data are not available.

Our pROI can be compared to other group ROIs on the FS average brain or can be projected to any individual brain using CBA to generate a predicted location of place-selective voxels in new individuals. We believe that this approach will be particularly useful in patient

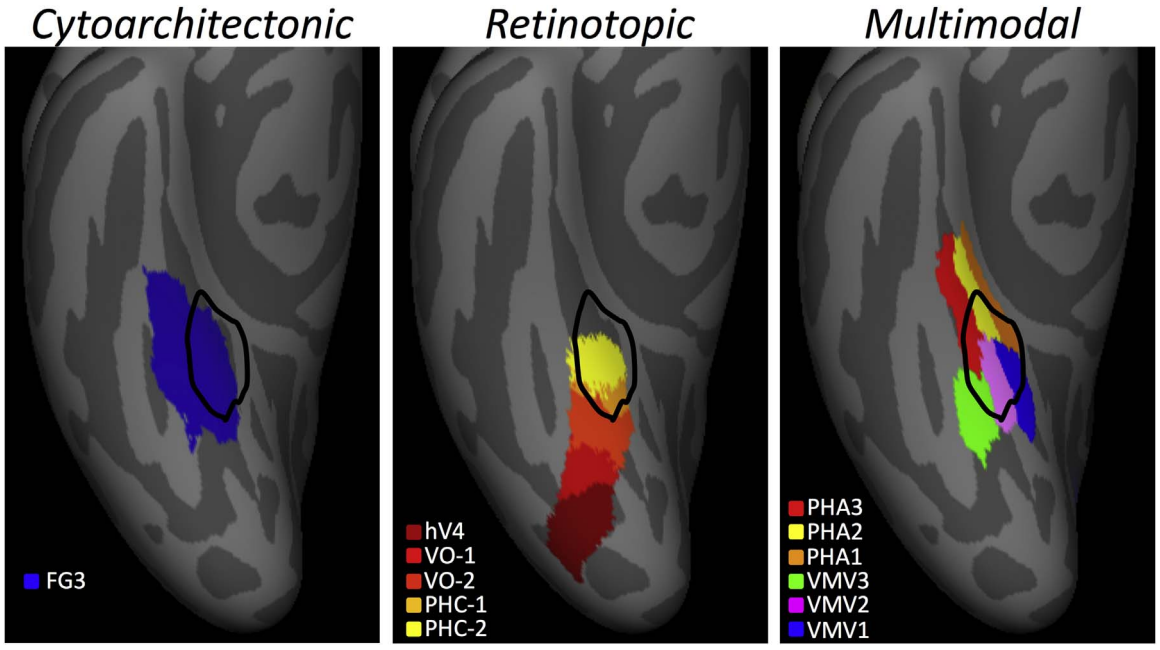

Fig. 6. pROI of place selectivity relative to probabilistic definitions of cytoarchitectonic, retinotopic, and multimodal parcellations of medial VTC. The FreeSurfer cortical surface zoomed in on ventral temporal cortex of the right hemisphere. *Black outline:* Contour of the place selectivity pROI from 24 subjects in the present study. *Left:* Blue: a maximum probability map of cytoarchitectonically defined area FG3 (Lorenz et al., 2017; Weiner et al., 2017). *Middle*: a maximum probability map of retinotopic areas within ventral occipitotemporal cortex (see legend for details; Wang et al., 2015). *Right*: a maximum probability map of regions within parahippocampal cortex determined by a recent multimodal parcellation technique (Glasser et al., 2016). FG3: fusiform gyrus 3; hV4: human visual area 4 (Brewer et al., 2005); PHA: parahippocampal area (Glasser et al., 2016); PHC: parahippocampal cortex; VMV: ventromedial visual (Glasser et al., 2016); VO: ventral occipital (Brewer et al., 2005).

populations (e.g. blind individuals; Amedi et al., 2007; He et al., 2013; Mahon et al., 2009; Wolbers et al., 2011) and intracranial studies (e.g. Bastin et al., 2013; Davidesco et al., 2013; Engell and McCarthy, 2010; Jacques et al., 2015; Megevand et al., 2014; Murphey et al., 2009; Rangarajan et al., 2014) in which it may not be possible to obtain fMRI data, but high resolution anatomical MRI data are typically obtained. Additionally, having a probabilistic ROI of place selectivity in typical adults can enable future studies to test differences across development (Cohen Kadosh and Johnson, 2007; Golarai et al., 2007; Peelen et al., 2009; Scherf et al., 2007; Gomez et al., 2017), lifespan (Park et al., 2012), or atypical populations (Aguirre and D'Esposito, 1999; Epstein et al., 2001; Golarai et al., 2006; Golarai et al., 2010a; Lind et al., 2013; Mendez and Cherrier, 2003).

Several anatomical and functional constraints likely contribute to the functional-structural coupling of place selectivity and cortical folding patterns

Based on the tight relationship between cortical folding and place selectivity in medial VTC measured in the present study, we hypothesize that white matter connectivity and underlying cytoarchitecture may impose constraints on the location of place selectivity in human medial VTC. Evidence that white matter connections may contribute to the location of the PPA comes from several recent studies that discovered white matter tracts in the ventral temporal lobe that are associated specifically with place selectivity (Gomez et al., 2015; Tavor et al., 2014; Saygin et al., 2012). Additionally, we recently quantified the relationship between the functional and cytoarchitectonic heterogeneity in VTC and found that place-selective voxels in medial VTC are largely contained within a single cytoarchitectonic area (FG3; Lorenz et al., 2017), which spans the CoS and medial FG (Weiner et al., 2017, see also Fig. 6). Furthermore, white matter tracts and underlying cytoarchitectonics associated with place selectivity in medial VTC are anatomically distinct from tracts and cytoarchitectonic areas associated with face selectivity in lateral VTC (Gomez et al., 2015; Tavor et al., 2014; Osher et al., 2015; Saygin et al., 2012; Weiner et al., 2016 Weiner et al., 2017). Thus, accumulating evidence indicates that long-range white matter connectivity and local cellular architecture likely contribute to the tight correspondence between place selectivity and cortical folding in human medial VTC.

Nevertheless, other empirical findings indicate that the PPA is not functionally or anatomically homogenous. For example, using a data-driven approach, Çukur and colleagues showed that the PPA contains differentiable voxel tuning for multiple semantic categories (Çukur et al., 2016). Additionally, Arcaro and colleagues showed that the PPA is retinotopically heterogeneous as it spans multiple retinotopic maps (Arcaro et al., 2009). Importantly, we replicate these findings at the group level: our pROI of place selectivity also spans several retinotopic maps as defined by Wang and colleagues (2015; see Fig. 6). Finally, comparing our pROI relative to a recent multimodal parcellation of the brain (Glasser et al., 2016) shows that our pROI contains portions of six different regions (Fig. 6). Based on the combination of these findings, at least two hypotheses may be tested in future studies: (1) anatomical constraints such as white matter connectivity and cytoarchitectonics may couple with place selectivity at the level of an area, while other anatomical features (for example, receptor architectonics (Caspers et al., 2015; Zilles et al., 2002, 2004) may correspond to more fine-grained functional distinctions (for example, semantics and retinotopy) or (2) there are additional subdivisions of both white matter and cytoarchitecture that correspond to functionally distinct subdivisions of the PPA/CoS-places. Future research combining in-vivo measurements of tissue properties (Dick et al., 2012; Glasser and Van Essen, 2011; Mezer et al., 2013; Gomez et al., 2017), white matter tracts, and functional properties within the same subjects may be useful to test these hypotheses as well as identify additional sources contributing to the structural-functional coupling in and around the PPA/CoS-places. Altogether, these data across studies suggest that a combination of anatomical and functional constraints contribute to the tight correspondence between place selectivity and cortical folding in medial VTC.

Conclusion

The present study shows that the location of place-selective voxels in medial VTC relative to cortical folding is so consistent that it could be predicted from a probabilistic ROI generated from independent groups of participants. These findings extend recent results showing that cortical positions of high-level visual areas in the ventral temporal lobe are reliably arranged relative to the macroanatomy. Our results are important because they reveal regularities in the functional organization of high-level visual cortex, which is contrary to the assumption that high inter-subject variability in functional-structural relationships is a general feature of the organization of higher sensory cortices at the level of areas. Importantly, our study provides a cross-validated method to accurately localize place selectivity in individual participants when fMRI data are not available.

Conflicts of interest

None.

Acknowledgements

Author contributions.

KW: designed the study, performed morphological analyses, defined fROIs in Study 1, generated pROIs, performed the statistical analyses, and wrote the manuscript.

MB: developed and implemented cortex based alignment tools, developed tools for the analytical pipeline across studies, and collected anatomical data used for morphological analyses.

NW, GG: collected data and defined fROIs from Study 2.

AS: collected data and defined fROIs from Study 1.

KNK: analyzed data from the Human Connectome Project.

JG, VN: collected anatomical data that were used for morphological analyses.

KA, KZ: collected and scanned the postmortem brains used for morphological analyses.

KGS: designed, oversaw these studies, and wrote the manuscript.

This research was funded by NEI grants 1 RO1 EY 02391501A1 and 1 RO1 EY 02231801A1, as well as funding from the European Union Seventh Framework Programme (FP7/2007–2013) under grant agreement no. 604102 (Human Brain Project). We thank Shahin Nasr for sharing data from his previously published work.

Appendix A. Supplementary material

Supplementary data associated with this article can be found in the online version at doi:10.1016/j.neuroimage.2017.04.040.

References

Aguirre, G.K., D'Esposito, M., 1999. Topographical disorientation: a synthesis and taxonomy. Brain 122 (Pt 9), 1613–1628.

Aguirre, G.K., Zarahn, E., D'Esposito, M., 1998. An area within human ventral cortex sensitive to "building" stimuli: evidence and implications. Neuron 21, 373–383.

Amedi, A., Stern, W.M., Camprodon, J.A., Bermpohl, F., Merabet, L., Rotman, S., Hemond, C., Meijer, P., Pascual-Leone, A., 2007. Shape conveyed by visual-to-auditory sensory substitution activates the lateral occipital complex. Nat. Neurosci. 10, 687–689.

Arcaro, M.J., McMains, S.A., Singer, B.D., Kastner, S., 2009. Retinotopic organization of human ventral visual cortex. J. Neurosci. 29, 10638–10652.

Avidan, G., Hasson, U., Hendler, T., Zohary, E., Malach, R., 2002. Analysis of the neuronal selectivity underlying low fMRI signals. Curr. Biol. 12, 964–972.

Baldassano, C., Beck, D.M., Fei-Fei, L., 2013. Differential connectivity within the parahippocampal place area. Neuroimage 75, 228–237.

Barch, D.M., Burgess, G.C., Harms, M.P., Peterson, S.E., Schlagger, B.L., Corbetta, M., Glasser, M.F., Curtiss, S., Dixit, S., Feldt, C., Nolan, D., Bryant, E., Hartley, T., Footer, O., Bjork, J.M., Poldrack, R., Smith, S., Johansen-Berg, H., Snyder, A.Z., Van Essen, D.C., WU-Minn HCP Consortium, 2013. Function in the human connectome: task-fmri and individual differences in behavior. NeuroImage 80, 169–189.

Bastin, J., Vidal, J.R., Bouvier, S., Perrone-Bertolotti, M., Benis, D., Kahane, P., David, O., Lachaux, J.P., Epstein, R.A., 2013. Temporal components in the parahippocampal place area revealed by human intracerebral recordings. J Neurosci. 33, 10123–10131.

Ben-Shachar, M., Dougherty, R.F., Deutsch, G.K., Wandell, B.A., 2007. Differential sensitivity to words and shapes in ventral occipito-temporal cortex. Cereb. Cortex 17, 1604–1611.

Benson, N.C., Butt, O.H., Brainard, D.H., Aguirre, G.K., 2014. Correction of distortion in flattened representations of the cortical surface allows prediction of V1-V3 functional organization from anatomy. PLoS Comput. Biol. 10 (3), e1003538.

Benson, N.C., Butt, O.H., Datta, R., Radoeva, P.D., Brainard, D.H., Aguirre, G.K., 2012. The retinotopic organization of striate cortex is well predicted by surface topology. Curr. Biol. 22 (21), 2081–2085.

Brewer, A.A., Liu, J., Wade, A.R., Wandell, B.A., 2005. Visual field maps and stimulus selectivity in human ventral occipital cortex. Nat. Neurosci. 8, 1102–1109.

Caspers, J., Palomero-Gallagher, N., Caspers, S., Schleicher, A., Amunts, K., Zilles, K., 2015. Receptor architecture of visual areas in the face and word-form recognition region of the posterior fusiform gyrus. Brain Struct. Funct. 220, 205–219.

Caspers, J., Zilles, K., Eickhoff, S.B., Schleicher, A., Mohlberg, H., Amunts, K., 2013. Cytoarchitectonical analysis and probabilistic mapping of two extrastriate areas of the human posterior fusiform gyrus. Brain Struct. Funct. 218, 511–526.

Cohen Kadosh, K., Johnson, M.H., 2007. Developing a cortex specialized for face perception. Trends Cogn. Sci. 11, 367–369.

Çukur, T., Huth, A.G., Nishimoto, S., Gallant, J.L., 2016. Functional subdomains within scene-selective cortex: parahippocampal place area, retrosplenial complex, and occipital place area. J Neurosci. 16 (6), 763–770.

Davidesco, I., Harel, M., Ramot, M., Kramer, U., Kipervasser, S., Andelman, F., Neufeld, M.Y., Goelman, G., Fried, I., Malach, R., 2013. Spatial and object-based attention modulates broadband high-frequency responses across the human visual cortical hierarchy. J Neurosci. 33, 1228–1240.

Dick, F., Tierney, A.T., Lutti, A., Josephs, O., Sereno, M.I., Weiskopf, N., 2012. In vivo functional and myeloarchitectonic mapping of human primary auditory areas. J Neurosci. 32, 16095–16105.

Dumoulin, S.O., Bittar, R.G., Kabani, N.J., Baker, C.L., Jr., Le Goualher, G., Bruce Pike, G., Evans, A.C., 2000. A new anatomical landmark for reliable identification of human area V5/MT: a quantitative analysis of sulcal patterning. Cereb. Cortex 10, 454–463.

Engell, A.D., McCarthy, G., 2010. Selective attention modulates face-specific induced gamma oscillations recorded from ventral occipitotemporal cortex. J Neurosci. 30, 8780–8786.

Epstein, R., 2008. Parahippocampal and retrosplenial contributions to human spatial navigation. Trends Cogn. Sci. 12 (10), 388–396.

Epstein, R., 2014. Neural systems for visual scene recognition. In: Bar, M., Keveraga, K. (Eds.), Scene Vision. MIT Press, Cambridge MA, 105–134.

Epstein, R., Deyoe, E.A., Press, D.Z., Rosen, A.C., Kanwisher, N., 2001. Neuropsychological evidence for a topographical learning mechanism in parahippocampal cortex. Cogn. Neuropsychol. 18, 481–508.

Epstein, R., Kanwisher, N., 1998. A cortical representation of the local visual environment. Nature 392, 598–601.

Fischl, B., Sereno, M.I., Tootell, R.B., Dale, A.M., 1999. High-resolution intersubject averaging and a coordinate system for the cortical surface. Hum. Brain Mapp. 8, 272–284.

Frost, M.A., Goebel, R., 2012. Measuring structural-functional correspondence: spatial variability of specialised brain regions after macro-anatomical alignment. Neuroimage 59, 1369–1381.

Glasser, M.F., Coalson, T.S., Robinson, E.C., Hacker, C.D., Harwell, J., Yacoub, E., 2016. A multi-modal parcellation of human cerebral cortex. Nature. 536, 171–178. http://dx.doi.org/10.1038/nature18933.

Glasser, M.F., Van Essen, D.C., 2011. Mapping human cortical areas in vivo based on myelin content as revealed by T1- and T2-weighted MRI. J Neurosci. 31, 11597–11616.

Glezer, L.S., Riesenhuber, M., 2013. Individual variability in location impacts orthographic selectivity in the "visual word form area". J Neurosci. 33, 11221–11226.

Glover, G.H., 1999. Simple analytic spiral K-space algorithm. Magn. Reson. Med. 42, 412–415.

Golarai, G., Ghahremani, D.G., Whitfield-Gabrieli, S., Reiss, A., Eberhardt, J.L., Gabrieli, J.D., Grill-Spector, K., 2007. Differential development of high-level visual cortex correlates with category-specific recognition memory. Nat. Neurosci. 10, 512–522.

Golarai, G., Grill-Spector, K., Reiss, A.L., 2006. Autism and the development of face processing. Clin. Neurosci. Res. 6, 145–160.

Golarai, G., Hong, S., Haas, B.W., Galaburda, A.M., Mills, D.L., Bellugi, U., Grill-Spector, K., Reiss, A.L., 2010a. The fusiform face area is enlarged in Williams syndrome. J. Neurosci. 30, 6700–6712.

Golarai, G., Liberman, A., Yoon, J.M., Grill-Spector, K., 2010b. Differential development of the ventral visual cortex extends through adolescence. Front. Hum. Neurosci. 3, 80 .

Golarai, G., Liberman, A., Grill-Spector, K., 2017. Experience shapes the development of neural substrates of face processing in human ventral temporal cortex. Cereb. Cortex 27 (2), 1229–1244.

Gomez, J., Barnett, M.A., Natu, V.S., Mezer, A., Palomero-Gallagher, N., Weiner, K.S., Amunts, K., Zilles, K., Grill-Spector, K., 2017. Growth of tissue in human cortex is coupled with the development of face processing. Science 355 (6320), 68–71.

Gomez, J., Pestilli, F., Witthoft, N., Golarai, G., Liberman, A., Poltoratski, S., Yoon, J., Grill-Spector, K., 2015. Functionally defined white matter reveals segregated pathways in human ventral temporal cortex associated with category-specific processing. Neuron 85, 216–227.

Grill-Spector, K., 2003. The neural basis of object perception. Curr. Opin. Neurobiol. 13, 1–8.
Grill-Spector, K., Malach, R., 2004. The human visual cortex. Ann. Rev. Neurosci. 27, 649–677.
Grill-Spector, K., Kushnir, T., Hendler, T., Malach, R., 2000. The dynamics of object-selective activation correlate with recognition performance in humans. Nat. Neurosci. 3 (8), 837–843.
Grill-Spector, K., Weiner, K.S., 2014. The functional architecture of the ventral temporal cortex and its role in categorization. Nat. Rev. Neurosci. 15, 536–548.
He, C., Peelen, M.V., Han, Z., Lin, N., Caramazza, A., Bi, Y., 2013. Selectivity for large nonmanipulable objects in scene-selective visual cortex does not require visual experience. Neuroimage 79, 1–9.
Henschen, S., 1893. On the visual path and centre. Brain 16, 170–180.
Huntgeburth, S.C., Petrides, M., 2012. Morphological patterns of the collateral sulcus in the human brain. Eur. J. Neurosci. 35, 1295–1311.
Huschke, E., 1854. Schaedel, Hirn und Seele des Menschen und der Thiere nach Alter, Geschlecht und Race, dargestellt nach neuen Methoden und Untersuchungen. Mauke, Jena.
Inouye, T., 1909. Die Sehstörungen bei Schussverletzungen der Kortikalen Sehsphäre nach Beobachtungen an Verwundeten der Letzten Japanischen Kriege. W. Engelmann, Leipzig, Germany.
Jacques, C., Witthoft, N., Weiner, K.S., Foster, B.L., Rangarajan, V., Hermes, D., Miller, K.J., Parvizi, J., Grill-Spector, K., 2015. Corresponding ECoG and fMRI category-selective signals in human ventral temporal cortex. Neuropsychologia..
Julian, J.B., Fedorenko, E., Webster, J., Kanwisher, N., 2012. An algorithmic method for functionally defining regions of interest in the ventral visual pathway. Neuroimage 60, 2357–2364.
Kay, K.N., Rokem, A., Winawer, J., Dougherty, R.F., Wandell, B.A., 2013. GLMdenoise: a fast, automatic technique for denoising task-based fMRI data. Front Neurosci. 7, 247.
Levy, I., Hasson, U., Avidan, G., Hendler, T., Malach, R., 2001. Center-periphery organization of human object areas. Nat. Neurosci. 4, 533–539.
Levy, I., Hasson, U., Harel, M., Malach, R., 2004. Functional analysis of the periphery effect in human building related areas. Hum. Brain Mapp. 22, 15–26.
Lind, S.E., Williams, D.M., Raber, J., Peel, A., Bowler, D.M., 2013. Spatial navigation impairments among intellectually high-functioning adults with autism spectrum disorder: exploring relations with theory of mind, episodic memory, and episodic future thinking. J. Abnorm. Psychol. 122, 1189–1199.
Lorenz, S., Weiner, K.S., Caspers, J., Mohlberg, H., Schleicher, A., Bludau, S., Eickhoff, S.B., Grill-Spector, K., Zilles, K., Amunts, K., 2017. Two new cytoarchitectonic areas on the human mid-fusiform gyrus. Cereb. Cortex. 27 (1), 373–385.
Mahon, B.Z., Anzellotti, S., Schwarzbach, J., Zampini, M., Caramazza, A., 2009. Category-specific organization in the human brain does not require visual experience. Neuron 63, 397–405.
Mangin, J.F., Auzias, G., Coulon, O., Sun, Z.Y., Riviere, D., Regis, J., 2015. Sulci as landmarks. In: Toga, A.W. (Ed.), Brain Mapping: An Encyclopedic Reference. Academic Press, New York.
Megevand, P., Groppe, D.M., Goldfinger, M.S., Hwang, S.T., Kingsley, P.B., Davidesco, I., Mehta, A.D., 2014. Seeing scenes: topographic visual hallucinations evoked by direct electrical stimulation of the parahippocampal place area. J. Neurosci. 34, 5399–5405.
Mendez, M.F., Cherrier, M.M., 2003. Agnosia for scenes in topographagnosia. Neuropsychologia 41, 1387–1395.
Mezer, A., Yeatman, J.D., Wandell, B.A., 2013. Quantifying the Local Tissue Volume and Composition in Individual Brains with MRI. Nat. Med..
Murphey, D.K., Maunsell, J.H., Beauchamp, M.S., Yoshor, D., 2009. Perceiving electrical stimulation of identified human visual areas. Proc. Natl. Acad. Sci. USA 106, 5389–5393.
Nasr, S., Echavarria, C.E., Tootell, R.B., 2014. Thinking outside the box: rectilinear shapes selectively activate scene-selective cortex. J Neurosci. 34, 6721–6735.
Nasr, S., Liu, N., Devaney, K.J., Yue, X., Rajimehr, R., Ungerleider, L.G., Tootell, R.B., 2011. Scene-selective cortical regions in human and nonhuman primates. J. Neurosci. 31, 13771–13785.
Nestares, O., Heeger, D.J., 2000. Robust multiresolution alignment of MRI brain volumes. Magn. Reson. Med. 43, 705–715.
Ono, M., Kubik, S., Abernathy, C.D., 1990. Atlast of the cerebral sulci. Thieme, New York.
Osher, D.E., Saxe, R.R., Koldewyn, K., Gabrieli, J.D., Kanwisher, N., Saygin, Z.M., 2015. structural connectivity fingerprints predict cortical selectivity for multiple visual categories across cortex. Cereb. Cortex..
Park, J., Carp, J., Kennedy, K.M., Rodrigue, K.M., Bischof, G.N., Huang, C.M., Rieck, J.R., Polk, T.A., Park, D.C., 2012. Neural broadening or neural attenuation? Investigating age-related dedifferentiation in the face network in a large lifespan sample. J. Neurosci. 32, 2154–2158.
Peelen, M.V., Glaser, B., Vuilleumier, P., Eliez, S., 2009. Differential development of selectivity for faces and bodies in the fusiform gyrus. Dev. Sci. 12, F16–F25.
Petrides, M., 2012. The Human Cerebral Cortex. Academic Press, New York.
Rangarajan, V., Hermes, D., Foster, B.L., Weiner, K.S., Jacques, C., Grill-Spector, K., Parvizi, J., 2014. Electrical stimulation of the left and right human fusiform gyrus causes different effects in conscious face perception. J. Neurosci. 34, 12828–12836.
Retzius, G., 1896. Das Menschenhirn. Studien in der makroskopischen Morphologie. Kgl. Buchdr. P. A. Norstedt and Söner, Stockholm.
Saygin, Z.M., Osher, D.E., Koldewyn, K., Reynolds, G., Gabrieli, J.D., Saxe, R.R., 2012. Anatomical connectivity patterns predict face selectivity in the fusiform gyrus. Nat. Neurosci. 15, 321–327.
Scherf, K.S., Behrmann, M., Humphreys, K., Luna, B., 2007. Visual category-selectivity for faces, places and objects emerges along different developmental trajectories. Dev. Sci. 10, F15–F30.
Silson, E.H., Steel, A.D., Baker, C.I., 2016. Scene-selectivity and Retinotopy in medial parietal cortex. Front. Hum. Neurosci. 10, 412.
Smith, G.E., 1907. New Studies on the Folding of the Visual Cortex and the Significance of the Occipital Sulci in the Human Brain. J. Anat. Physiol. 41, 198–207.
Stigliani, A., Weiner, K.S., Grill-Spector, K., 2015. Temporal processing capacity in high-level visual cortex is domain-specific. J. Neurosci. 35 (36), 12412–12424.
Talairach, J., Tournoux, P., 1988. Co-Planar Stereotaxic Atlas of the Human Brain: 3-dimensional Proportional System—an Approach to Cerebral Imaging. Thieme, New York.
Tavor, I., Yablonski, M., Mezer, A., Rom, S., Assaf, Y., Yovel, G., 2014. Separate parts of occipito-temporal white matter fibers are associated with recognition of faces and places. Neuroimage 86, 123–130.
Tootell, R.B., Mendola, J.D., Hadjikhani, N.K., Ledden, P.J., Liu, A.K., Reppas, J.B., Sereno, M.I., Dale, A.M., 1997. Functional analysis of V3A and related areas in human visual cortex. J. Neurosci. 17, 7060–7078.
Vu, A.T., Gallant, J.L., 2015. Using a novel source-localized phase regressor technique for evaluation of the vascular contribution to semantic category area localization in BOLD fMRI. Front. Neurosci. 9, 411.
Wandell, B.A., Chial, S., Backus, B.T., 2000. Visualization and measurement of the cortical surface. J. Cogn. Neurosci. 12, 739–752.
Wandell, B.A., Rauschecker, A.M., Yeatman, J.D., 2012. Learning to see words. Annu. Rev. Psychol. 63, 31–53.
Wang, L., Mruczek, R.E.B., Arcaro, M.J., Kastner, S., 2015. Probabilistic maps of visual topography in human cortex. Cereb. Cortex, 1–21.
Weiner, K.S., Barnett, M.A., Lorenz, S., Caspers, J., Stigliani, A., Amunts, K., Zilles, K., Fischl, B., Grill-Spector, K., 2017. The cytoarchitecture of domain-specific regions in human high-level visual cortex. Cereb. Cortex 27 (1), 146–161.
Weiner, K.S., Jonas, J., Gomez, J., Maillard, L., Brissart, H., Hossu, G., Jacques, C., Loftus, D., Colnat-Coulbois, S., Stigliani, A., Barnett, M.A., Grill-Spector, K., Rossion, B., 2016. The face processing network is resilient to focal resection of human visual cortex. J Neurosci. 36 (32), 8425–8440.
Weiner, K.S., Golarai, G., Caspers, J., Chuapoco, M.R., Mohlberg, H., Zilles, K., Amunts, K., Grill-Spector, K., 2014. The mid-fusiform sulcus: a landmark identifying both cytoarchitectonic and functional divisions of human ventral temporal cortex. Neuroimage 84, 453–465.
Weiner, K.S., Grill-Spector, K., 2010. Sparsely-distributed organization of face and limb activations in human ventral temporal cortex. Neuroimage 52, 1559–1573.
Weiner, K.S., Grill-Spector, K., 2011. Not one extrastriate body area: using anatomical landmarks, hMT+, and visual field maps to parcellate limb-selective activations in human lateral occipitotemporal cortex. Neuroimage 56, 2183–2199.
Weiner, K.S., Grill-Spector, K., 2012. The improbable simplicity of the fusiform face area. Trends Cogn. Sci. 16, 251–254.
Weiner, K.S., Grill-Spector, K., 2013. Neural representations of faces and limbs neighbor in human high-level visual cortex: evidence for a new organization principle. Psychol. Res. 77, 74–97.
Weiner, K.S., Sayres, R., Vinberg, J., Grill-Spector, K., 2010. fMRI-adaptation and category selectivity in human ventral temporal cortex: regional differences across time scales. J. Neurophysiol. 103, 3349–3365.
Weiner, K.S., Zilles, K., 2016. The anatomical and functional specialization of the fusiform gyrus. Neuropsychologia 83, 48–62.
Wilder, B.G., 1901. Brain. In: Buck, A.H. (Ed.), A Reference Handbook of the Medical Sciences. William Wood and Company, New York.
Witthoft, N., Nguyen, M.L., Golarai, G., LaRocque, K.F., Liberman, A., Smith, M.E., Grill-Spector, K., 2014. Where is human V4? Predicting the location of hV4 and VO1 from cortical folding. Cereb. Cortex 24, 2401–2408.
Wolbers, T., Klatzky, R.L., Loomis, J.M., Wutte, M.G., Giudice, N.A., 2011. Modality-independent coding of spatial layout in the human brain. Curr. Biol. 21, 984–989.
Yeatman, J.D., Rauschecker, A.M., Wandell, B.A., 2013. Anatomy of the visual word form area: adjacent cortical circuits and long-range white matter connections. Brain Lang. 125, 146–155.
Zilles, K., Palomero-Gallagher, N., Grefkes, C., Scheperjans, F., Boy, C., Amunts, K., Schleicher, A., 2002. Architectonics of the human cerebral cortex and transmitter receptor fingerprints: reconciling functional neuroanatomy and neurochemistry. Eur. Neuropsychopharmacol. 12, 587–599.
Zilles, K., Palomero-Gallagher, N., Schleicher, A., 2004. Transmitter receptors and functional anatomy of the cerebral cortex. J Anat. 205, 417–432.